DEVICE DESIGN FOR IN-SITU EIS MEASUREMENTS OF ORGANIC COATINGS UNDER ACCELERATED DEGRADATION VIA IMPINGEMENT FLOW

A Paper
Submitted to the Graduate Faculty
of the
North Dakota State University
of Agriculture and Applied Science

By

Quan Yuan

In Partial Fulfillment of the Requirements
for the Degree of
MASTER OF SCIENCE

Major Department:
Mechanical Engineering

December 2019

Fargo, North Dakota

North Dakota State University
Graduate School

Title

Device Design for In-Situ EIS Measurements of Organic Coatings under Accelerated Degradation via Impingement Flow

By

Quan Yuan

The Supervisory Committee certifies that this ***Paper*** complies with North Dakota State University's regulations and meets the accepted standards for the degree of

MASTER OF SCIENCE

SUPERVISORY COMMITTEE:

Dr. Yechun Wang
Chair

Dr. Long Jiang

Dr. Zhibin Lin

Approved:

12/31/2019
Date

Dr. Allan R. Kallymeyer
Department Chair

ABSTRACT

This paper demonstrated a holistic approach to the study of corrosion degradation mechanism of organic coatings using impingement flows. A state-of-the-art impingement flow testing device was developed for the experimental investigations of coating degradation behavior under various fluid flow conditions. The testing device employed Electrochemical Impedance Spectroscopy (EIS) to monitor and quantify the coating performance. This study prepares us for a pathway to investigate the degradation mechanism of coatings using both mechanistic and electrochemical approaches. This paper provided a limited amount of experimental data to show the capability of the current experimental setup. A pigmented marine coating was tested under a 90-degree jet impingement flow of a looped 3.5% wt. NaCl solution. The measured impedance results indicated that the coating barrier property decreased for all tested flow rates. It was also found impingement flow can accelerate the coating degradation process comparing with the standard stationary immersion tests.

ACKNOWLEDGEMENTS

"If I have seen further, it is only by standing on the shoulders of giants."

-Issac Newton

Firstly, I would like to thank my graduate advisor, Dr. Yechun Wang, for her unwavering guidance, wisdom, and patience throughout my master`s study endeavor. This paper and my graduate study could not have been completed without her support. I am also grateful for the personal growth, insights, and life experiences gained from her that are far beyond the scope of this paper.

Secondly, I would not be able to complete my graduate school experience without the love and support of both sides of my family. Thank you all for the tremendous support and caring over the years.

Finally, I would like to thank Dr. Long Jiang and Dr. Zhibin Lin for being on my committee and their recommendation for my paper. I also would like to thank the faculties, friends, and all those who have helped me during my student life at North Dakota State University. Your contributions made this experience invaluable and thank you all for being part of this great journey.

DEDICATION

This paper is dedicated to my wife Linh Hoang, who is always bringing love, support, courage, and care to me during the thick and thin of my life.

TABLE OF CONTENTS

LIST OF FIGURES

INTRODUCTION

Objective

Corrosion has a significant economic and social impact on our society. Among all the corrosion prevention techniques, applying organic coatings is a conventional but one of the most cost-effective methods. Organic coatings generally perform well and can have a long service life. However, they tend to degrade within their working environment over time. Thus, understanding the degradation mechanism of coatings and predicting its service life is crucial for both corrosion prevention and coating development. Coating performance studies usually employ accelerated testing techniques to determine the quality of the coatings. In real life, corrosion is not only the result of the electrochemical reaction but also can be influenced by fluid flow. The fluid flow over the coatings can accelerate the degradation process of coatings. Hence, the coating degradation induced by a fluid flow would be a great topic to investigate. This work focuses on the device design of an impingement flow system. This impingement flow system can generate different flow conditions. With Electrochemical Impedance Spectroscopy (EIS) measurement device, it can monitor the organic coating corrosion degradation mechanism under the impingement flow characteristics. Due to the fluid flow that can accelerate this corrosion process, this setup is also an accelerated testing technique. This device is crucial for the evaluation of organic coating performance.

The organization of this paper contains five sections. The first section gives the basic introduction of corrosion and corrosion prevention methods. The second section offers the theory support of impingement flow and Electrochemical Impedance Spectroscopy (EIS). The third section is the literature review, and it provides the current progress on the organic coating degradation study under impingement flow by using the EIS technique. The fourth section

focuses on the device design. After that, experimental data is presented in the results and discussion section. The final section is for the conclusion and future work.

Corrosion

Corrosion has been an inevitable part of our daily lives. Corrosion is generally considered as the wastage of a metal due to the action of corrosive agents. However, the broad definition of corrosion is the degradation of material through contact with its environment. Corrosion commonly takes place on metallic materials. Nevertheless, it can also be found on non-metallic materials such as concrete and plastics [1]. This study focused on the corrosion of organic coatings that are employed to protect metallic substrates.

The deterioration process of metallic material caused by corrosion is mostly from an electrochemical reaction. This reaction usually comes in the form of metal oxidation. It takes place at the interface between the exposed metal surface and its environment. Three necessary conditions to facilitate corrosion to occur are metallic materials, oxygen, and electrolytes. Based on the differences in the environments, corrosion researchers and engineers categorize corrosion into atmospheric corrosion, aqueous corrosion, and soil corrosion. Besides, based on the failure mechanisms, corrosion can be classified into general attack corrosion, localized corrosion, galvanic corrosion, environmental cracking, flow-accelerated corrosion, intergranular corrosion, dealloying, fretting corrosion, high-temperature corrosion. It is sporadic to see the corroding structure only under a single corrosion mechanism. In this study, flow-accelerated corrosion in an aqueous environment is the focus.

Since the fluid flow can affect the nature, number, and peak intensity of the chemical species of the corrosion process [2]. Flow-accelerated corrosion has a corrosion mechanism in which the fluid flow damages the protective layer on the metal surface. Therefore, it creates an

opportunity for the underlying metal substrate to have contact with water, oxygen, and ions to initiate corrosion.

Flow-accelerated Corrosion

Fundamental researches covered on the topic of flow-accelerated corrosion can be dated back to at least three decades ago. Corrosion researchers and engineers have investigated the corrosion mechanism under various flow types and hydrodynamics conditions. These findings improved our understanding of the corrosion mechanism. The learnings from these studies also promoted the creation of corrosion detection technologies as well as the development of corrosion prevention products and processes.

Many studies used a mechanistic approach to describe the conjoint relationship between fluid flow and corrosion. Heitz classifies four main types of flow-accelerated corrosion. They are classified as mass transport controlled corrosion, phase transport controlled corrosion, erosion-corrosion, and cavitation corrosion [3] shown in Figure 1.

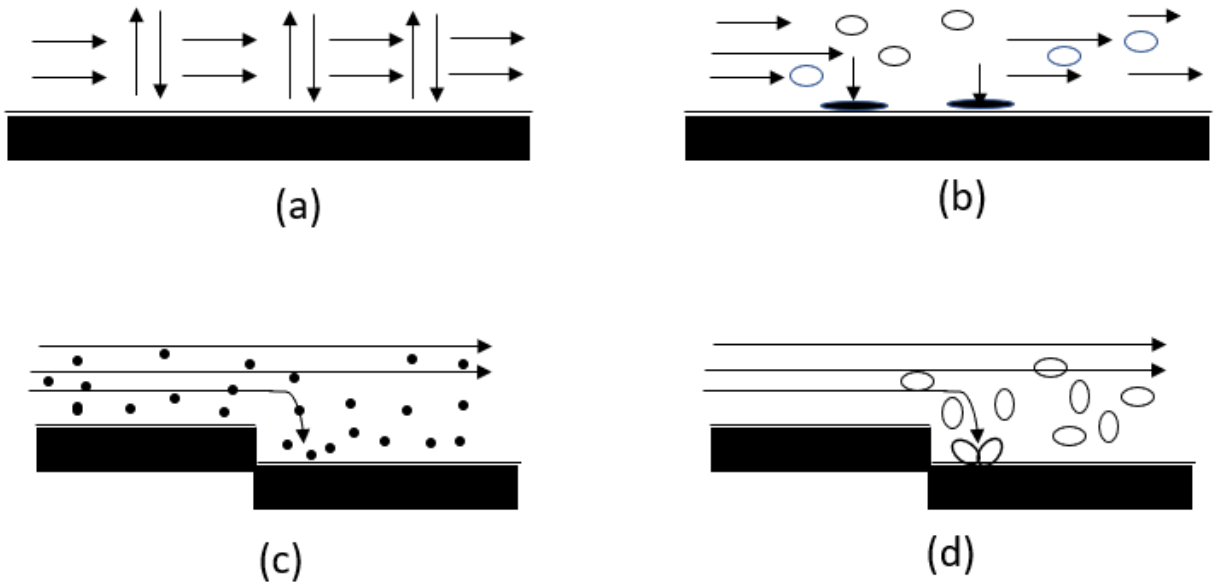

Figure 1. Four main mechanisms of flow-accelerated corrosion: (a) mass transport-controlled corrosion (b) phase transport corrosion (c) erosion-corrosion (d) cavitation corrosion [3]

Mass transport-controlled corrosion is a relatively uniform type of corrosion. A convective diffusion layer locates near the fluid-solid interface. The rate of convective mass transfer determines the overall corrosion rate. Mass transport-controlled corrosion governs the actual electrochemical process. Mass transfer-controlled corrosion tends to have a smooth surface finish on the corroded area. Phase transport corrosion has a wetting of the metal surface by a corrosive phase. The phase caused the wetting of the metal, and it contains the corrosive agent is the determinant. The corroded area usually tends to be a rough surface. Erosion corrosion is a result of combined effects between the mechanical forces from the fluid flow and the electrochemical process at the liquid-solid layers. For a liquid flow, the mechanical forces are typically from shear stress within the high-velocity turbulence region or the impact of abrasive elements. The surfaces affected by erosion-corrosion sometimes have shallow pits, or other local phenomena depends on the flow direction. When the vapor bubbles explode in a fluid flow near the liquid-solid interface, it causes a sudden change of pressure, can cause cavitation corrosion. The implosion produced by these vapor bubbles can remove the protective surfaces when the flow velocity of fluid flow changes, disruptions, or alterations in the flow direction can also cause cavitation due to the hydro-mechanical effects. The surface morphology of cavitation corrosion appears as a series of closely spaced sharp-edged pits or craters.

Implication of Corrosion

Corrosion has a significant impact on the global economy. According to the National Association of Corrosion Engineers (NACE), the annual global cost due to corrosion is estimated at around $ 2.5 trillion. It is equivalent to 3.4% of the global GDP [4]. For the U.S. alone, the cost due to corrosion exceeds $1 trillion for the first time in 2013. Corrosion affects three primary economic sectors globally: services, industry, and agriculture. In the U.S., the corrosion

cost to the industry sector accounts for nearly 20% of the entire cost of corrosion. Besides, the metallic corrosion impacts nearly every U.S. industry sector [5]. The above figures are merely a direct cost of corrosion to our economy. For the indirect cost caused by corrosion such as plant downtime, loss of product, loss of efficiency, environmental contaminations, structure failures, overdesigned products would generate even a much higher cost to our economy [6].

Flow-accelerated corrosions commonly exist in off-shore and marine technologies, oil and gas production, and of the processes within energy industries. It can cause wall thinning of carbon steel piping, tubing, and vessels. Once the wall thickness reaches the critical thickness required for supporting the operating stresses, it can lead to catastrophic failure of the component. Flow-accelerated corrosion is a significant mode of failure for pipelines in the oil industry [7]. Furthermore, flow-accelerated corrosion can cause damages to the pumps, impellers, valves, heat exchanger tubes, and other hydraulic types of equipment and also to components used in the process industries [3]. Wei et al. studied the corrosion degradation behavior of a fusion-bonded epoxy powder coating system under both the flowing and static 3% NaCl aqueous solution. The experimental results indicated that the flowing condition aggravated the deterioration of coatings [8].

Corrosion Prevention

Although the cost due to corrosion is enormous, the corrosion process could still be preventable or at least delayed. According to the National Association of Corrosion Engineers (NACE), applying corrosion prevention practices can create significant global savings of up to 35 percent of the cost of corrosion damage. It is an equivalent saving of $375-875 billion per year [4]. Corrosion can be prevented by using many techniques, including painting/coating, sacrificial anode, cathodic protection, and natural products of corrosion itself. However, no

matter which types of corrosion prevention is chosen, the prevention strategies should be dependent on the type of mechanism concerned. This study emphasizes on the organic coating prevention method.

Organic Coatings

For corrosion prevention, applying organic coating is one of the most cost-effective modes for metallic objects and structures [9]. It functions as both decoration and protection [10]. Organic coating creates a barrier between the underlying metal substrate from its environment. This barrier can reduce the amount of transportation of oxygen, water, and ions significantly. Hence, this substrate receives protection [11]. Organic Coatings can also provide cathodic protection when pigmented with active metals or can passivate surfaces [12]. Corrosion prevention type of organic coatings, in general, has a very long service lifetime. For example, modern coatings used by the Bureau of Reclamation have service lives of 20–25 years. In contrast, some of the legacy coatings that contained red lead and chromate pigments had a service life of over 50 years [13]. The failure modes of organic coatings on the metal substrate is a complicated process and it is typically hard to give a substantial answer. However, it can be generalized into three main processes: (1) the transportation of water and ionic species across the coating films; (2) the creation of anodic and cathodic at the solid and liquid interface; (3) the defects within the coatings, the delamination, or the compositional changes of organic coatings [14]. Sometimes, the failure mode is a result of the combined process listed above. Therefore, understand the protection mechanism of coating and predict coating service life will be beneficial to develop better coating formulations and rank the performance of organic coatings.

Organic Coating Corrosion Testing Methods

Corrosion test is required for organic coating research and manufacturing. The two main findings when conducting a corrosion test on the organic coating: coating performance and service life prediction. Ranking the coating performance and develop better coatings becomes feasible with these results. There are currently two main approaches to test the performance of organic coatings: filed or service testing and laboratory testing.

Field or Service Testing

Field or service testing is a reliable coating performance evaluation method. Most of the field test is done on-site. However, the measurements of the residual coating properties could be performed within a laboratory environment after extensive exposure tests. The advantage of field testing is that the material sample is exposed and tested within a real working environment. The downside of field testing is very costly in time. The duration of some field testing could take many years. For example, zinc-coated metal samples need to test for more than 30 years. Some of the field tests are destructive, which means it must damage the organic coatings to be able to get the coating performance data.

Laboratory Testing

Almost every type of corrosion test can be performed in a laboratory environment. Typically, accelerated testing methods of organic coatings are prevalent to conduct [15]. There are many types of acceleration tests on coatings. These tests are performed by increasing the exposure time and intensity to temperature, light, moisture and humidity, mechanical stresses, and even environmental pollutants [16][17][18][19]. The principle for accelerated testing on organic coating is to apply a coating failure stress that is generally at a much higher intensity than that in real-life situations. As a result, coating fails in a relatively shorter time. The most

crucial part of accelerated testing is that the failure mechanism should stay the same as the failure mechanism in a real-life situation. The commonly used accelerated testing methods for organic coatings are the salt fog chamber test, QUV test, thermal cycling test, and cyclic wet-dry test [20][21][22][23]. One of the standard accelerated coating testing methods is salt-fog testing under the ASTM B117 [24].

THEORY AND METHODS

This chapter discusses the theory of impingement flow and the hydrodynamic characteristics associated with it. Besides, the theory used in Electrochemical Impedance Spectroscopy (EIS) and its relevance to the components of the coating system is also introduced here.

Types of Impingement Flow

Impingement flow can be classified into two main groups: free-surface flows and submerged flow shown in Figure 2 [25]. For the submerged impingement flow, it is typically defined as the impinging jets exuding into a reservoir that contains the same liquid as the impinging jet. This study focuses on the submerged impingement flow.

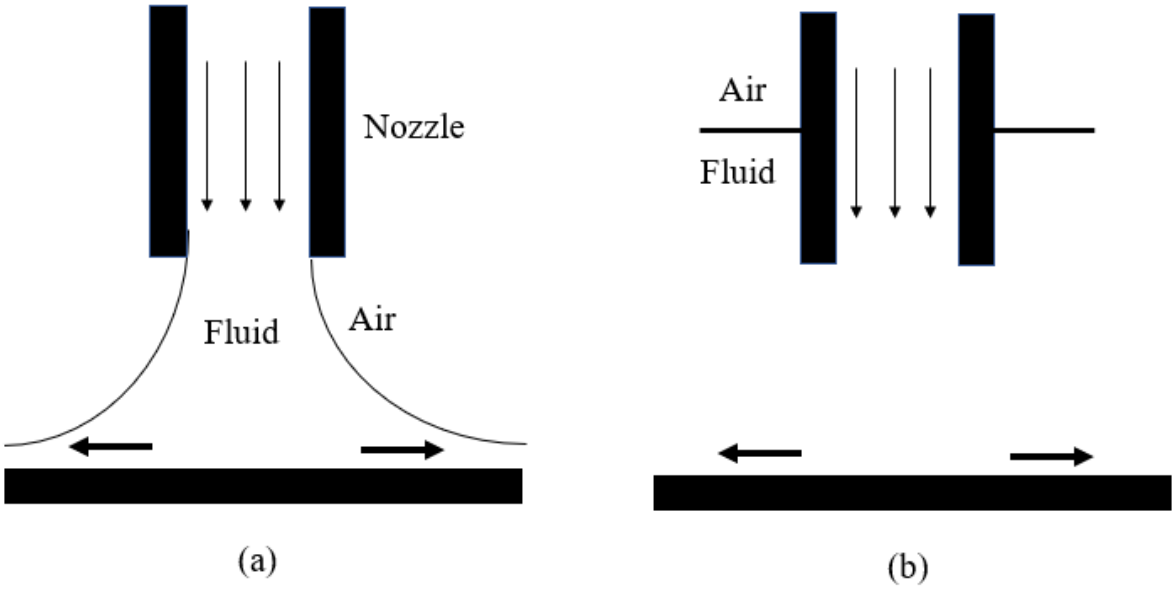

Figure 2. Different types of impingement flows: (a) free surface flow (b) submerged flow [25]

For the submerged impingement flow system, the impinging jet and the stagnant fluid together can create turbulence in the transition zone which is near the fluid-solid wall interface shown in Figure 3 [26].

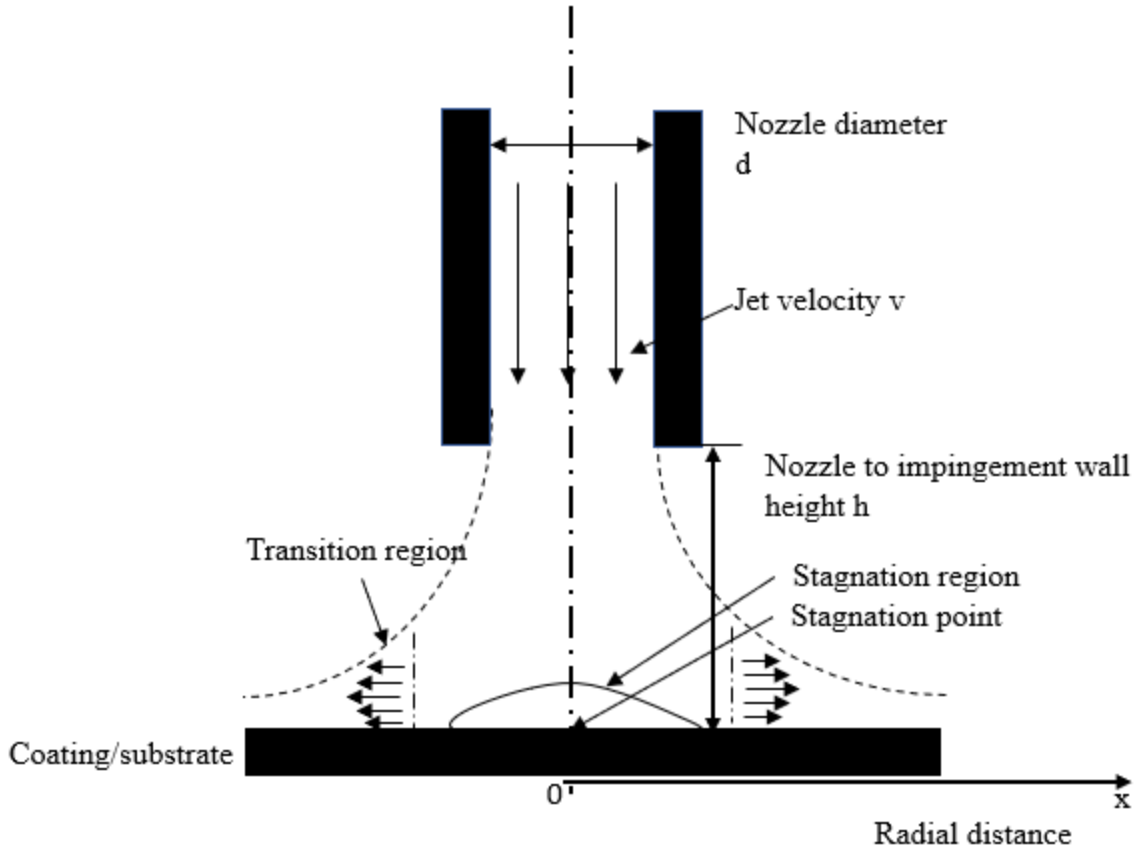

Figure 3. Schematic of the flow regimes of a submerged, normal impinging jet flow [26]

The flow characteristics of an impinging jet on a flat surface usually have three major zones: the laminar zone, the high turbulence transition zone, and the low turbulence wall jet zone shown in Figure 4. A hydrodynamic boundary layer is also formed. In Efird's study [27], there are a diffusion boundary layer and viscous layer within this hydrodynamic layer.

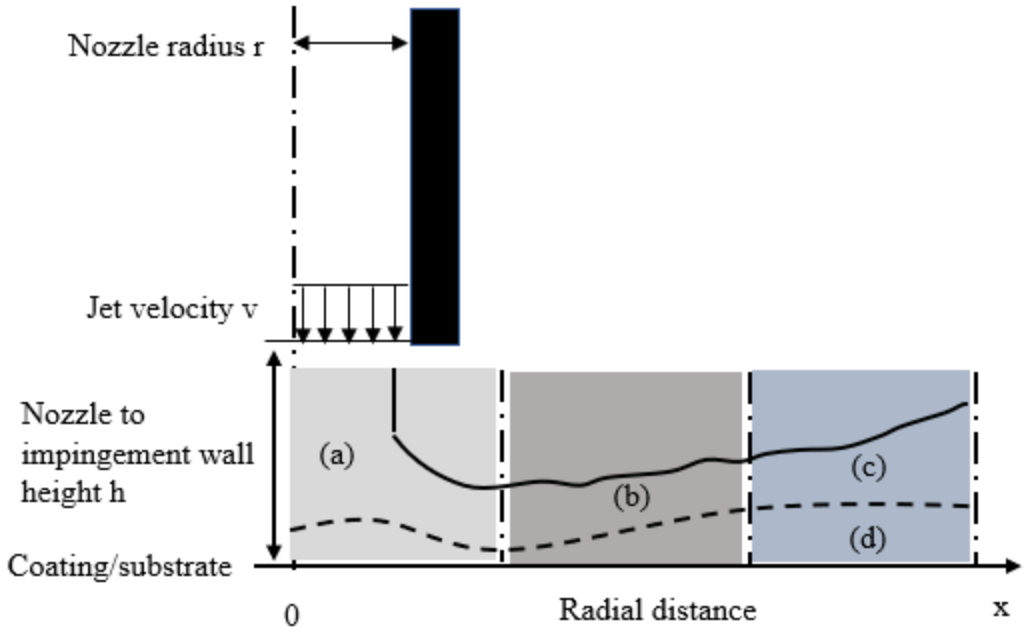

Figure 4. Hydrodynamic characteristics of a jet impinging on a flat surface: (a) laminar region (b) high turbulence transition region (c) low turbulence wall jet region (d) hydrodynamic boundary layer [27]

Impingement Flow Wall Shear Stress

The wall shear stress induced by the impingement flow is a significant factor. It is directly related to the viscous energy loss within the fluid boundary layer. Wall shear stress represents the intensity of drag in the fluid, acting on the fluid-solid interface. Efird [27] believes shear stress can represent the intensity of turbulence in the fluid as well. The total shear stress in a fluid past a fixed wall is the combination of the viscous and the Reynolds stresses [27]. Nevertheless, Reynolds' stress becomes zero at the wall. The wall shear stress is expressed as,

$$\tau_w = v(\frac{\partial U}{\partial y})_{y=0}$$

Where, U is flow velocity, and v is the dynamic viscosity of the fluid.

For impingement flow, shear stress is a function of fluid velocity, radial position, and critical radius [28]. Giralet and Trass derived the equation for the wall shear stress in an impinging jet as the function of the radial distance from the centerline [29]. The expression is,

$$\tau_w = 0.179\ \rho V^2 Re^{-0.182}(\frac{r}{r_0})^{-2}$$

Where Re is Reynolds number and it can predict the whether the flow is laminar or turbulent, $\frac{r}{r_0}$ is the ratio between impinging jet nozzle diameter and radial distance on the wall to the center of the jet line.

Impingement Flow Mass Transfer

The mass transfer coefficient in the diffusion layer has a direct influence on the flow-induced corrosion, an expression of the mass transfer coefficient rate shows as the following,

$$k_d = \frac{D_J}{\delta_d}$$

Where, D_J is the diffusion coefficient for species J. δ_d is the diffusion boundary layer thickness.

Electrical Impedance Theory

The simple concept of electrical resistance is defined as the ability of a circuit to resist the flow of current. It obeys Ohm`s law. However, many electrical systems in the real world show much more complex behavior, and we are using impendence to measure an electrical circuit`s tendency to resist the flow of an alternating electrical current. The mathematical expression for impedance Z is

$$\mathrm{Z} = \mathrm{V_{ac}}/\mathrm{I_{ac}}$$

Impedance definition: it is like resistance but has a broader application to the real world. It follows Ohm`s law at all current and voltage levels. Its resistance value is independent of frequency. It requires AC current and voltage signals through a resistor are in phase with each

other. It is usually measured by applying an AC potential to an electrochemical cell and then measuring the current through the cell. The potential excitation is typically in the sinusoidal form [30]. Therefore, the response to this potential is an AC current signal also in a sinusoidal form. For the expression of impedance is shown in the following,

$$Z = \frac{E_t}{I_t} = \frac{E_0 \sin(\omega t)}{I_0 \sin(\omega t + \emptyset)} = Z_0 \frac{\sin(\omega t)}{\sin(\omega t + \phi)}$$

Where, Z_0 is the magnitude of impedance, and ϕ is the phase shift. The impedance is a complex number,

$$Z(\omega) = \frac{E}{I} = Z_0 \exp(j\phi) = Z_0(\cos\phi + jsin\phi)$$

There are two ways to present the impedance data: Nyquist plot and Bode plot. For the Nyquist plot, the real portion of the impedance value is plotted on the X-axis, and the imaginary part is plotted Y-axis. On a Nyquist plot, the higher frequency data is plotted on the right side, and low-frequency data was plotted on the left side. The inconvenient side of EIS is that it cannot tell what frequency the data was recorded. Another way to present the impedance is by using the Bode plot. The advantage of the Bode plot is it shows the relationship between the impedance and frequency.

Electrochemical Impedance Spectroscopy (EIS)

Electrochemical Impedance Spectroscopy (EIS) is a powerful technique for studying a complicated system that involves electrochemistry [30]. Impedance data is measured, and it stands for the resist tendency of an alternating electrical current. A fully defined impedance requires the magnitude, phase angle, and frequency.

EIS has been widely used to predict the service lifetime of corrosion protective coatings, rank the coatings systems, and measure the water uptake in coatings. EIS data are also analyzed to develop meaningful models to analyze the physical behavior of coating degradation [31].

An electrochemical impedance instrument typically consists of a potentiostat, associated electronics to measure the impedance, and an electrochemical cell to contain the sample**.** Typically, an electrochemical cell is composed of three electrodes, working, counter, and the reference electrode. For EIS measurements of coatings, the working electrode connects to the metal substrate, a platinum mesh is employed as the counter electrode and saturated calomel electrode is used as the reference electrode.

The significant advantage of using EIS is that it can sensitively measure the deterioration of organic coating before any other detection methods. For example, before any discoloration or cracking takes place, EIS measurement data would show substantial changes. Besides, EIS data could be interpreted by equivalent circuit models that would help us to explain the physics of coating degradation. Also, EIS has the advantage of being able to combine with flow acceleration device to provide in-situ monitoring for the degradation of organic coatings.

LITERATURE REVIEW

Many studies focused on the shear stress of impingement flow and its impact on the corrosion rate. In Efird`s work, he found that shear stress contributes to corroding species movement within the viscous and diffusion boundary layers [27]. Wang et al. studied the corrosion mechanism of magnesium (Mg) alloys (MgZnCa) plates and AZ31 stents) under different fluid flow conditions representative of the vascular environment. The flow shear stress accelerates the overall corrosion (including localized, uniform, pitting and erosion corrosions) is because of the increased mass transfer and mechanical force [32]. Zhang and Cheng experimented with micro-electrodes flush-mounted on X65 pipeline steel to study the shear stress effect caused to corrosion under impingement flow. Moreover, the surface morphology result indicated the shear stress thinned and even removed the scale. Hence, it increased the corrosion rate. The highest corrosion rate on the microelectrodes is found to be the center where has the highest flow velocity and shear stress [33]. Demoz and Dabros studied the shear stress controlled-corrosion at the impinged jet wall of a pipe, they found the shear stress on the impinged jet wall increased radially at giving stagnation and jet wall region in the order of 2 and 2.9 times the jet radius, respectively. The jet-impinged wall shear stress at all radical position was 5-120 times that at the pipe wall at any given Reynold number [26]. Zhou et al. found that the flowing fluid enhanced the release of coating materials from the coating surface into the surrounding working fluid and the fluid shear stress decreased the thickness of coatings [31].

Some other researches focused on the angle of attack of impingement flows. Hukovic et al. studied the corrosion resistance of copper-nickel alloy under a 90-degree impingement flow at a different flow velocity of impingement flow. They found out increased fluid velocity results in a decrease in corrosion resistance, which was measured by Electronic Impedance Spectroscopy

measurements [34]. Toor et al. studied the effect angle variation on the corrosion performance of carbon steel in a flow loop, and with/without solid particles. These results suggested at 45 degree of impact angle the corrosion rate was the highest. Toor believes this was due to a balance between the shear and normal impact stress at this angle. The synergistic effect at 45-degree and the 90-degree angle was more significant as compared to the other angles [35]. It was also found a high mass loss on the uncoated sample at a low impact angle of silica-containing impingement flow [36]. This was also proved by Zhang and Cheng also investigated the impact angle of impingement jet on the microelectrodes flush mounted to the jet wall. They found the fluid flow velocity and shear stress, and the corrosion rate of the micro-electrodes shows a higher value at the location far away from the nozzle than those at the side close to the nozzle at the oblique impact angles. The corrosion behavior of the steel electrode located at the center of the sample holder generally increases when the impact angle decreases due to the enhancing shear effect on the corrosion scale [33]. Zhou et al. also found that the flowing rate of the working fluid has a significant influence on the degradation rate of organic coatings [37]. The local shear stress decreased with the increasing of Reynold number and tended to converge at a higher value of Reynold number. It was also found that shear stress was a function of the ratio between the impact height and radial distance [38].

Fluid flow is a significant contributor to the corrosion rate. Toor et al. also looked at the impingement flow velocity effect on the corrosion rate of metals. The result showed that the corrosion rate increases with an increase in the impingement flow velocity. It was found that the corrosion product or oxide layer was not stable under these high flow velocity conditions, which resulted in more material loss [35]. Jiang et al. studied the performance of corrosion inhibitors under the effect of flow velocity and found the critical flow velocity is different between

inhibitors [39]. Erosion-corrosion has been studied in many pieces of research and applying small particles in the working fluid can have significant impact on corrosion rate as well as coating performance [40], [41],[42].

Many studies utilized Electrochemical Impedance Spectroscopy (EIS) to evaluate coating performance [43]. It is the most used technique to evaluate the protective properties of coatings on a metal substrate. EIS on coating studies has been widely received and has a significant advantage over traditional testing techniques when measuring a complex system, especially has a low corrosion rate [44].

Shreepathi et al. used EIS to predict the service life of organic coatings in a C4-type environment, and he found that EIS could detect the initiation of corrosion earlier than the visual defects appeared [45]. Using the EIS technique can also help rank the performance of organic coating [46]. For flow accelerated corrosion, Zhou et al. used EIS to study flow accelerated the degradation of the organic clear coating immersed in laminar flows[31]. Chen et al. utilized EIS to study the inhibition performance of corrosion inhibitors in turbulent flow conditions [47].

A lot of these focused on the corrosion rate of the metal substrate, instead of that of organic coatings [39][48][49][50][51]. The existing work on coating degradation employed laminar flow without considering flow impingement. In addition, EIS was not utilized in those studies on impingement flow's effect on corrosion. In this paper, we have designed and set up a device that can use EIS to correlate the coating degradation with the flow characteristic of the impingement flow system. In this way, we could understand the mechanism of organic coating degradation and predict the service life of coatings under impingement flow.

Any experiment designed to measure coating quality must include a mechanism to stress the coating and induce its failure. By making periodic EIS measurements during the stress

process, a rate of coating failure can be estimated. EIS is a nondestructive measurement. This study enables researchers to study the coating deterioration process in a function of time and hydrodynamic characteristics.

There are two main approaches to study the organic coating degradation: from the hydrodynamic characteristics of the flow: try to correlate the shear stress and mass transfer coefficient to the corrosion rate. The second approach is using EIS to study the deterioration process. If we can combine both methods, that will help us to get a better understanding of the degradation behavior and corrosion mechanism.

IMPINGEMENT FLOW SYSTEM DEVICE DESIGN

Design Intent

This design intends to build an impingement flow system to study the degradation mechanism of organic coatings under the following influences of a wholly submerged impingement flow:

1. The influence of flow velocity of impingement flow
2. The influence of shear stress of impingement flow
3. The influence of mass transfer rate of impingement flow
4. The influence of impact angles of impingement flow
5. The influence of the fluid composition of impingement flow

Design Considerations

When designing this impingement flow system, many design considerations have been adapted to ensure the functionality and robustness of the final design. Since this study relates to the impingement flow system, this system must provide an apparatus to generate continuous, consistent, and controlled impingement jet flows to meet the testing needs. Coating corrosion degradation tests usually require some time to complete. Therefore, the entire impingement flow system should be capable of running continuous tests without any interruption until the failure of organic coatings.

Since the flow velocity affects many fluid characteristics, this system should include a pump that can provide a range of flow rates. Also, flow nozzles should be utilized to generate a fluid flow. The flow nozzles should offer a range of sizes and are interchangeable. Multiple different testing cells at the same or different impact angles should be designed because this will

meet the needs of performing several tests at once. Besides, organic coatings under the impact of different impingement jet angles can be studied.

The components used for building this design cannot be corroded, and particularly those parts which have direct contact with the working electrolyte. For example, the gauges used to measure the flow rate and flow pressure should not be corroded at any time. Furthermore, the working electrolyte should flow within an enclosed loop system to prevent any external contamination. Since Electrochemical Impedance Spectroscopy (EIS) is used to quantify the coating performance, this system should offer an enclosed space that is free of electromagnetic noise. Besides, there is a coating sample requirement when using EIS. The area of study for the coating needs to be within the range of 10 cm^2 to 30 cm^2 for the goal of getting a higher probability of exhibiting a defect in the coating, and a large electrode area will exhibit higher currents than a smaller area. A static immersion test on coatings is also required as a benchmark test. This system should be designed to perform dynamic, static, and combined cyclic impingement flow tests. Also, this system should allow the usage of different types of fluid flows, such as deionized water, salted water, or even fluid with small particles.

Experimental Setup

An impingement flow system was designed and built specifically for this experimentation shown in Figure 5. It consists of air diffuser, reservoir, pump driver and pump head, flowmeters, pressure gauges, testing cell, Faraday cage, Electrochemical Impedance Spectroscopy (EIS), and data acquisition system (DAQ). The actual experimental setup is shown in Figure 6.

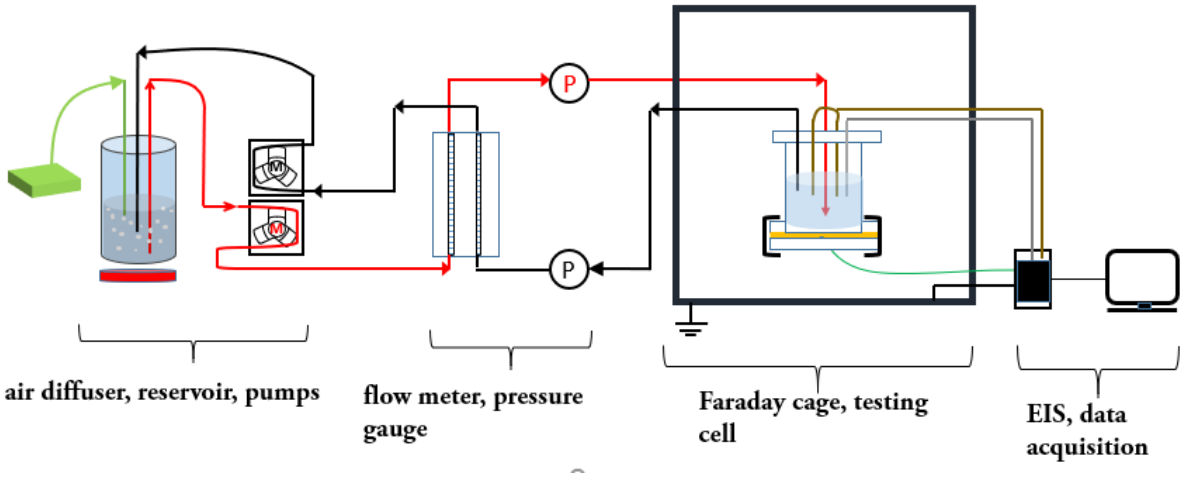

Figure 5. Impingement flow experimental setup

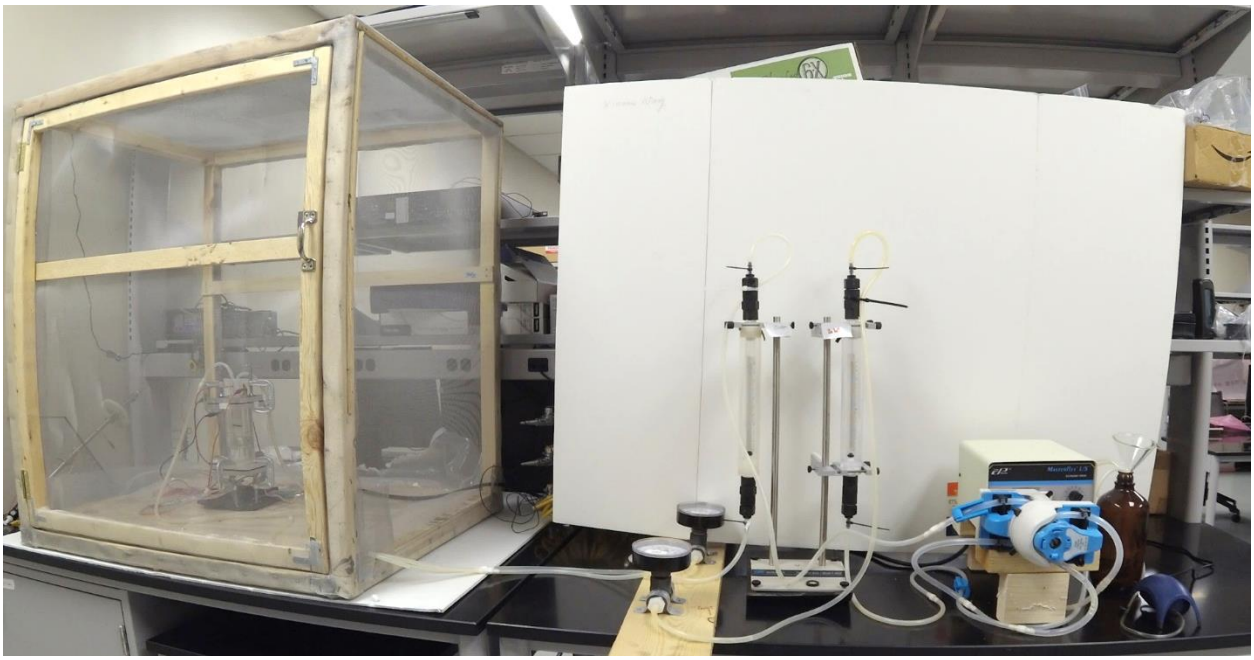

Figure 6. A picture of the impingement flow system

Apparatus

For the apparatus used for building this impingement flow system, the Electrochemical Impedance Spectroscopy (EIS) and its controlling software were realized by a computerized PCI4 300 EIS measurement device made by Gamry Instruments shown in Figure 7.

Figure 7. A picture of computerized Gamry PCI4 EIS 300 instrument [52]

For the pump system, the pump driver was a Masterflex L/S 7554-90 series pump driver along with a Materflex easy-load three pump heads. The pump has an adjustable RPM (20-600) to achieve various flow rates. For the tubing used in this entire system, it was provided by Masterflex, and the gauge is L/S 16.

Faraday cage

In order to achieve high-quality EIS measurements, the environmental electronic noise at low current should not be picked up by the system. A Faraday cage is a grounded conductive enclosure that reduces current noise received by the working electrode and voltage noise received by the reference electrode. The EIS testing cell must be placed in the Faraday cage

during the measurement. For this study, the Faraday cage was constructed by a fine steel mesh and 2x2 wood blocks shown in Figure 8. The overall sizes of the Faraday cage is 3 ft x 3ft x 3ft.

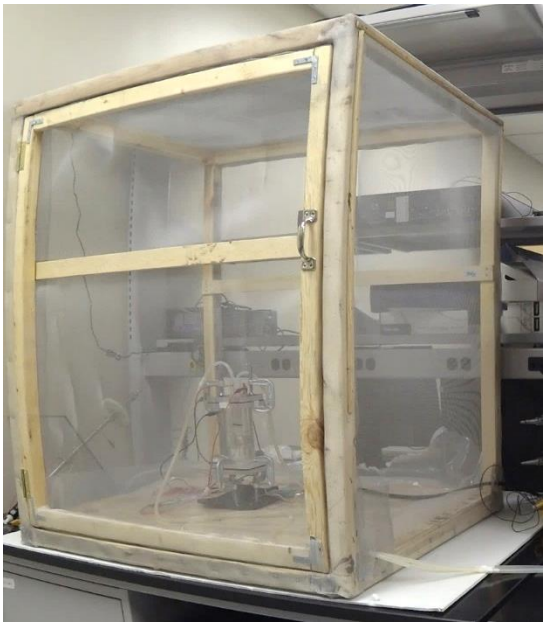

Figure 8. A picture of Faraday cage

Three main things need to be considered while building a Faraday cage. First, the Faraday cage should be covered by metal mesh in all six faces and block the external electronic noise. Second, the Faraday cage should include access for cables, tubes, and other wirings. The Faraday cage should also include a ground wire. Last but not least, the faraday cage should be big enough to allow multiple testing cells to fit inside as well as providing the visibility to allow the testers to check the progress of the organic coatings.

Electrochemical testing cell

A testing cell is where the actual coating testing takes place under the impingement flow. It is a piece of apparatus that holds organic coating samples in place under a submerged impingement flow to constant strike the system shown in Figure 9. For this study, a testing cell was crafted from polycarbonate. It consists of a cylinder tube with glued on top and bottom covers and separated top and bottom covers. For the cylinder tube, it has 2 inches of inner

diameter and 4 inches of height. The outer diameter is about 2.2 inches. It is not only corrosion-free but also can provide a transparent look for easy observation during the testing process. The testing cell has access for the nozzles, inlet tubes, outlet tubes, electrodes. The bottom plate of the testing cell has a CNC machined circle-shaped groove shown in Figure 10. Its depth is 1/16 of an inch. The purpose of this is to fit an O ring so that there will be a great seal during the testing process. Besides, a 30 degree and 60-degree testing cell were made by using polycarbonate shown in Figure 11.

Figure 9. Testing cell for the 90-degree impingement flow

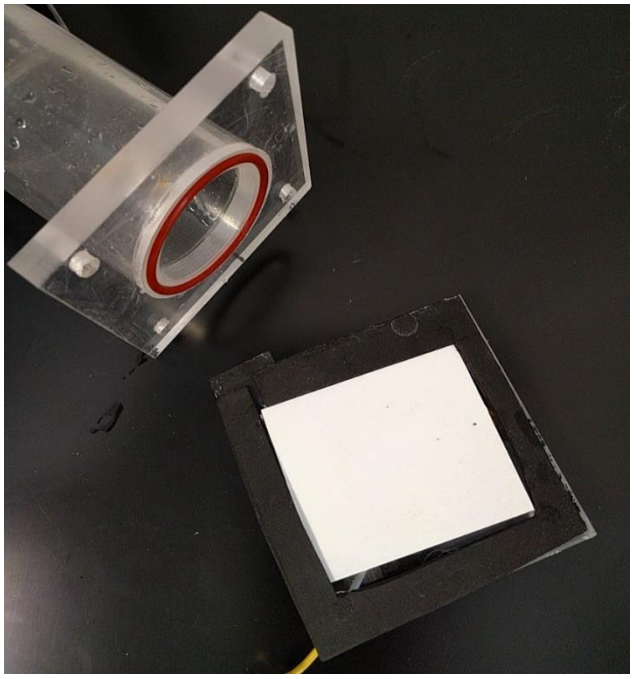

Figure 10. A picture of the bottom testing cell O-ring and coating sample

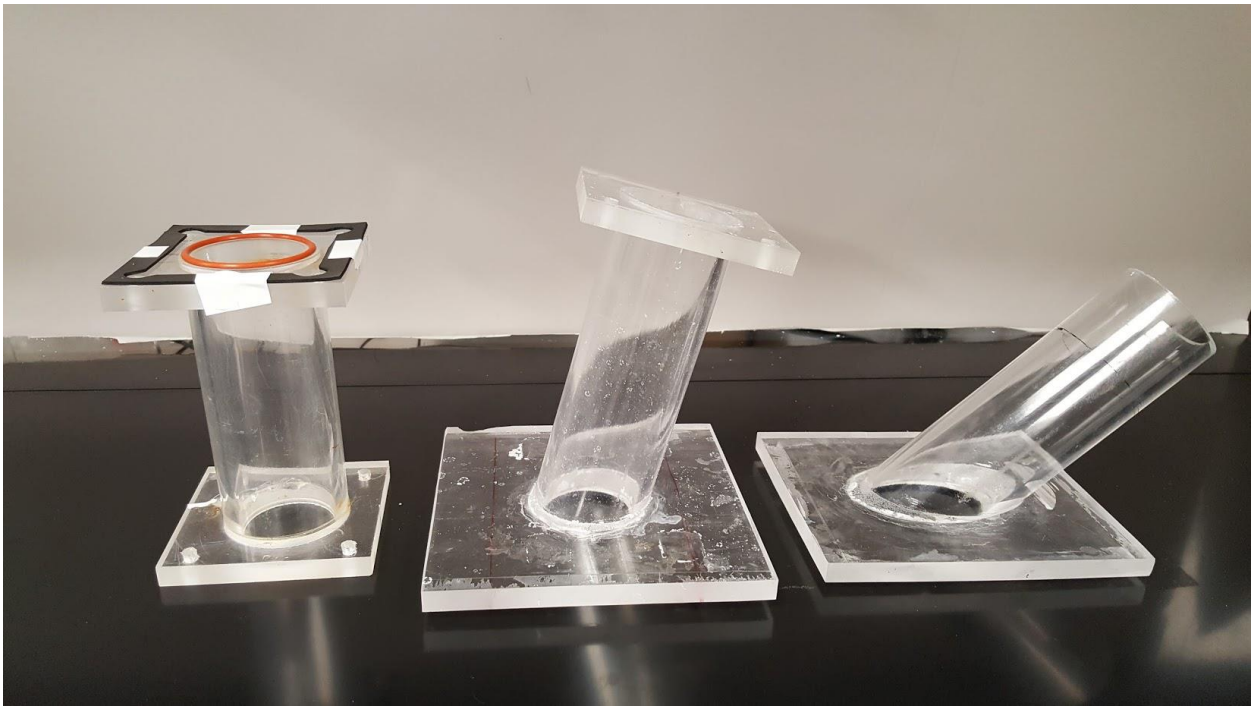

Figure 11. A picture of a 90-degree testing cell, 60-degree testing cell, and 30-degree testing cell

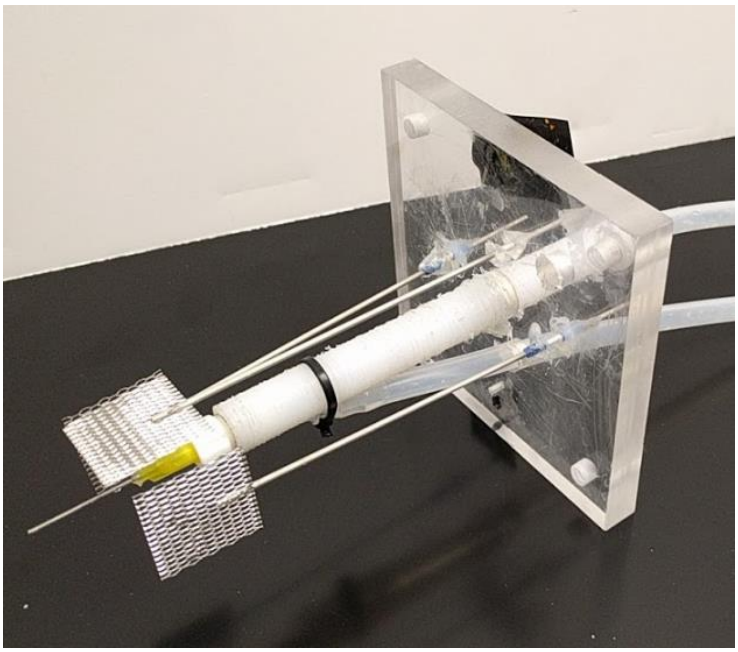

Figure 12. A picture of electrodes, nozzle, and inlet and outlet flow tubings

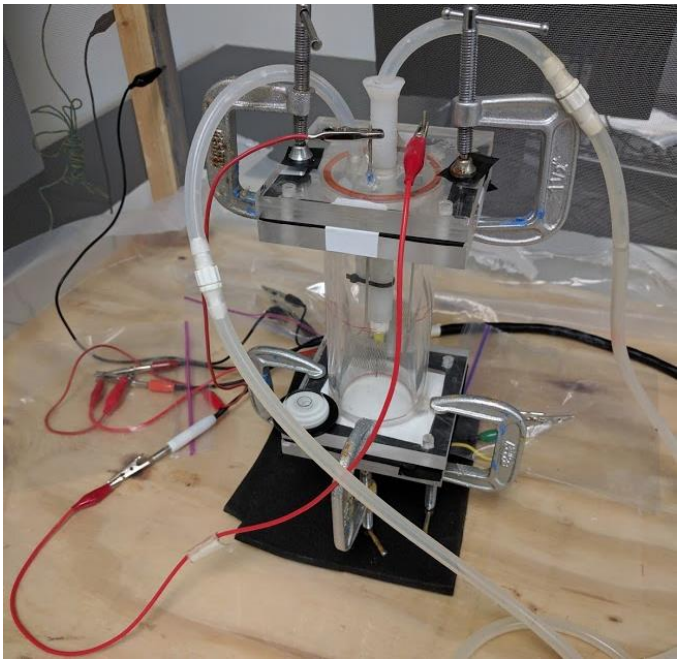

Figure 13. A picture of the entire testing cell assembly

Electrodes

The three-electrode setup was used for this apparatus. The metal substrate of the coating sample serves as a working electrode. As counter electrodes, a pair of platinum meshes were

used on the left and right sides of the impinging jet flow nozzle shown in Figure 13. A third platinum electrode is acting as the reference electrode.

Working fluid

The working fluid is a 3.5 wt% NaCl solution. It was prepared by dissolving NaCl powder into deionized (DI) water.

Flowmeter

Two Gilmont flowmeters with glass ball inside were used. One is used for measuring inlet flow velocity, and the other one is used for measuring outlet flow velocity. Both are needed to be calibrated regularly to ensure accurate readings.

Peristaltic driver and pump heads

The peristaltic pump has a unique design. It has a drive system that turns a set of rollers that compress and release flexible tubing as they rotate. A vacuum that was created by the squeezing action draws fluid through the tubing. The advantage of the peristaltic pump is that the working liquid is no longer in contact with the internal structure of the pump. Hence, there will be no corrosion contamination from the pumps.

Pump tubing

The pump Tubing used here is specialized for the Masterflex pump driver and head. It is an L/S 16-gauge tubing from Masterflex.

Working fluid reservoir

The working fluid reservoir is a glass container with lids that has access to the inlet and outlet tubing.

Air diffuser

An oxygen air diffuser has been used to pump oxygen into the working fluid reservoir. It ensures the oxygen is saturated inside of the working fluid during the test.

Elcometer

The thickness of the coating sample was measured by using an Elcometer 415 coating thickness gauge before and after the impingement tests. This thickness measurement was explicitly measured in the active region on the coating sample. This measurement was conducted at room temperature.

Gloss measurements

The gloss of the coating surface was evaluated by using a NovoTrio statistical gloss meter before and after the impingement tests. Gloss is an indication of surface smoothness. Typically, the higher gloss value indicates a much smoother surface finish. The gloss measurements conducted for all tested samples are based on three different grazing angles: 20°, 60°, and 85°. This measurement was conducted at room temperature.

Testing Procedure

For the testing procedure, it generally takes three primary steps: the first primary step is to prepare the coating samples and perform pre-measurement tests on these samples. The second primary step is to set the EIS devices and running the tests for an extended time. Lastly, the third step is to measure coating sample properties after the submersion is completed and to analyze EIS data

The organic coating sample fitted in this setup should be applied on a fabricated S-36 Q-panel, which is purchased from Q-Panel Lab Products. The fabricated Q-panel size is 2-inch x 2-inch. The organic coating was sprayed onto these fabricated Q-panels and get fully cured based

on the manufacturer's instruction. For this study, the organic coating used was the chlorinated rubber-based primer with pigmented aluminum flakes, and the topcoat is aliphatic polyester polyurethane resin shown in Figure 14.

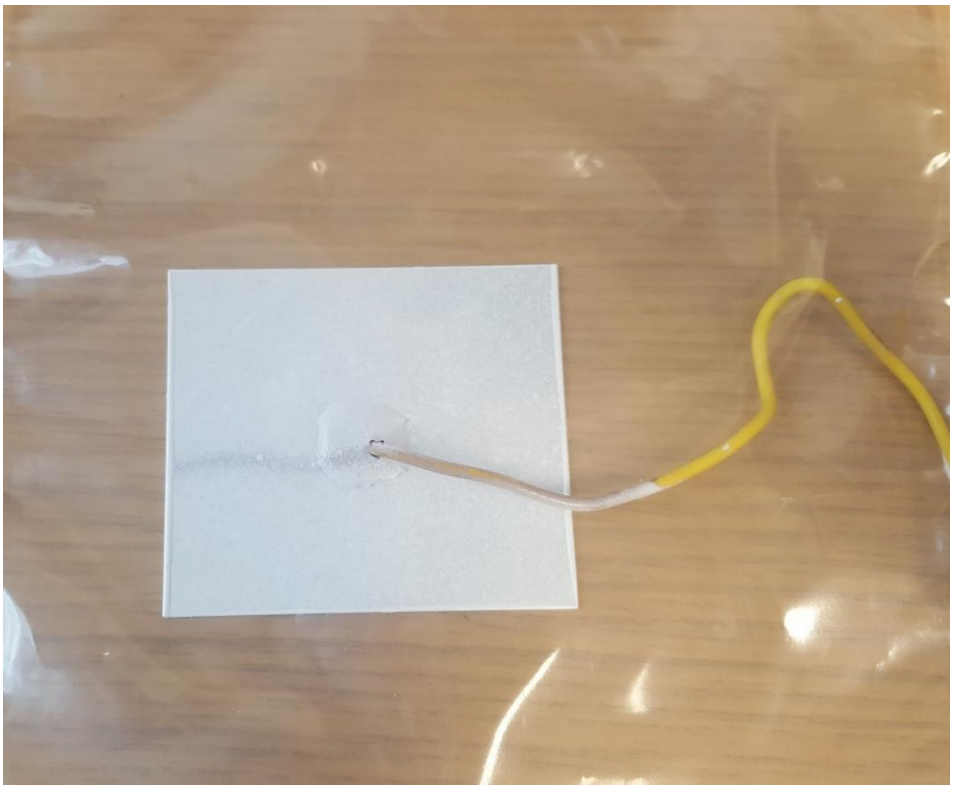

Figure 14. A picture of testing coating sample and the attached working electrode

For the coating sample preparation, the organic coating samples should be prepared at least 24 hours before the test to ensure the coating sample gets fully cured. Please refer to the manufacturer's instruction for curing time and plan ahead of time. In order to utilize the testing setup in this study, the organic coating should be applied to a fully prepared steel Q-panel to ensure proper adhesion. For the pre-test, steps are described in the following: First, polish the Q-panel with 320 grits of sandpaper then move onto a 600 grits sandpaper. Then the polished Q-panel should be cleaned with acetone and hexane and then let it air dry. Designated liquid paints are spray-coated on the Q-panel at the recommended air pressure to the prepared side of Q-panel uniformly in a spraying booth.

After the spray, the sprayed panels are cured at room temperature for at least 24 hours or follow the manufacturer's instruction. The next step is to attach a wire to the center of the uncoated side of the panels. Then epoxy is applied to the connection region to ensure the enclosure fully.

The following ASTM testing methods on organic coatings are recommended to perform but has to base on the specific needs: D1640 drying time, D3363 pencil hardness, D5402 MEK double rubs, D4366 König pendulum hardness, D465 acid number, D2794 impact resistance, D522 mandrel bend test (conical), D3359 adhesion by tape test (crosshatch), D523 gloss, D2369 non-volatile content, D1545 viscosity by bubble tube (Gardner-Holdt viscosity), D2196 Brookfield viscosity. For the required coating sample measurements, at least six measurements of coating thickness are performed with an electrometer at different locations of panels then find out the average value. The gloss values are measured with NovoTrio statistical gloss meter. The weight of each coating panel could be measured before and after the test if the weight-loss of coatings is of interest.

Pre-test check-up list and EIS setting

For the EIS setting, the scanning frequency range should be set from 10^{-2} to 10^{5} Hz with 10 points per decade with 15 mV AC perturbation coupled with the open circuit potential. EIS measurements were carried out every day during the immersed period. The data harvesting can be set automatic by using a sequencing method within the controlling software.

Then the next step is to check the flow system to ensure there is no overflow or any leakage. Fill the reservoir with a working fluid. Use the ultrasonic cleaner as a reservoir if the working fluid is nanofluid. Turn on the pump. Check the display of rotameter and pressure gauge to ensure each gauge is appropriately working. Adjust pump driver speed to achieve the required

and consistent flow rate and flow pressure. Start to run the EIS data recording. Adjust the flow rate and repeat the test and four coated samples need to be tested for the same flow condition.

Post-test coating measurement data analysis

Perform the thickness and gloss measurement on coatings after the test. For the EIS data, the Nyquist and Bode plot should be investigated. Then the impedance data can be used to generate equivalent circuit models.

RESULTS AND DISCUSSION

Coating degradation under the influence of flow velocity has been investigated in this study. For all the flow rates, the impedance modulus decreased with the immersion time shown in Figure 15 and Figure 16. The higher the flow rate, the coating impedance drops at a much faster speed.

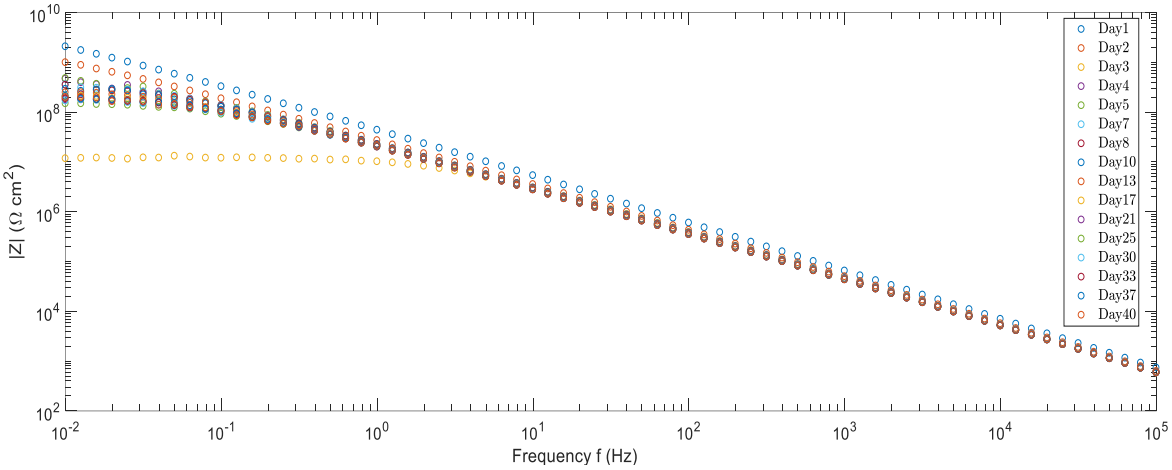

Figure 15. Impedance modulus as a function of frequency for coating samples under 90-degree 3.5% NaCl impingement flow at a flow rate of 3.683 cm^3/s

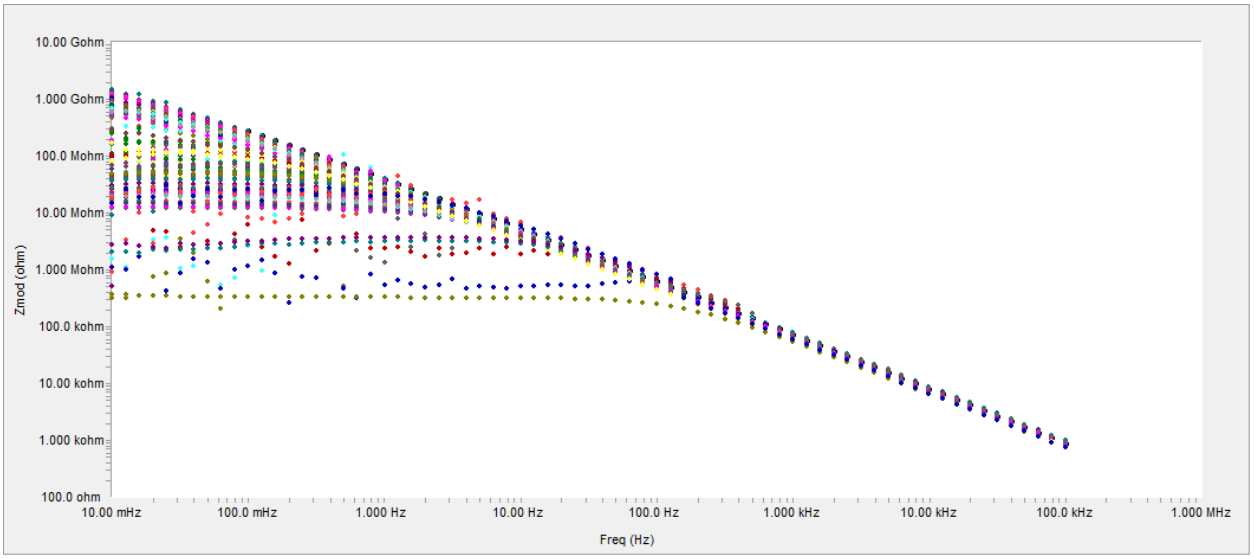

Figure 16. Impedance modulus as a function of frequency for coating samples under 90-degree 3.5% NaCl impingement flow at a flow rate of 5.233 cm^3/s

Based on the coating study, at low frequency, the impedance serves as a reliable indicator of the corrosion resistance of coating samples. Here in Figure 17, the impedance value at a frequency of 0.01 Hz has been plotted against time for the impingement flow at 3.683 cm^3/s under a 90 degree of impact. The result indicates this tested coating lost at least half of the corrosion resistance capability within 200 hours of the continuous experiment.

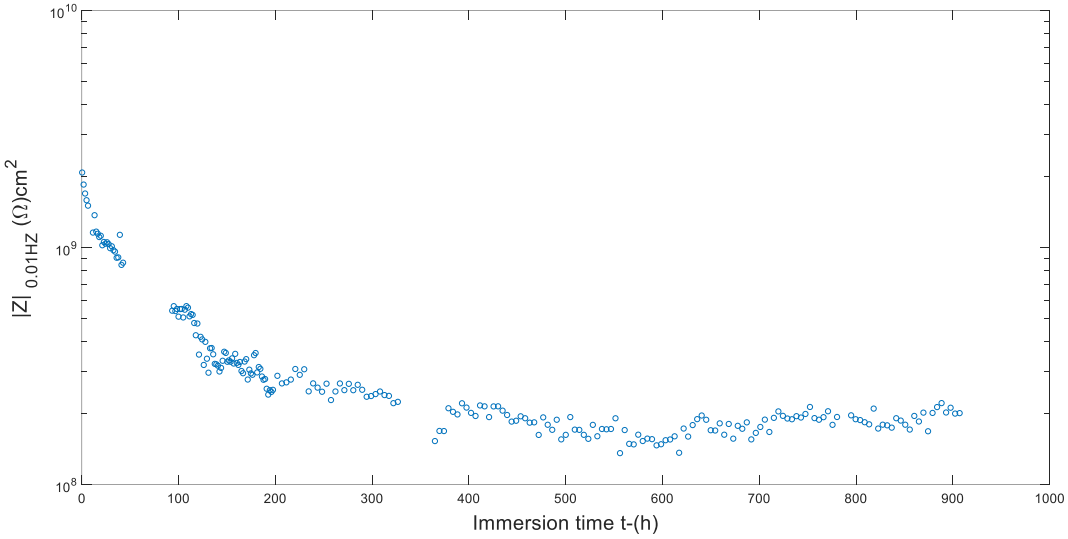

Figure 17. Organic coating sample under 90-degree impingement flow at a flow rate of 3.683 cm^3/s

In order to further understand the coating capability, it is reasonable to assume the first several data points represent the coating performance at its highest. In other words, the coating resistance is the highest upon immersion. From here, the impedance measurements are normalized based on the first data point. In Figure 18, an overview of coating protective capability over time is provided.

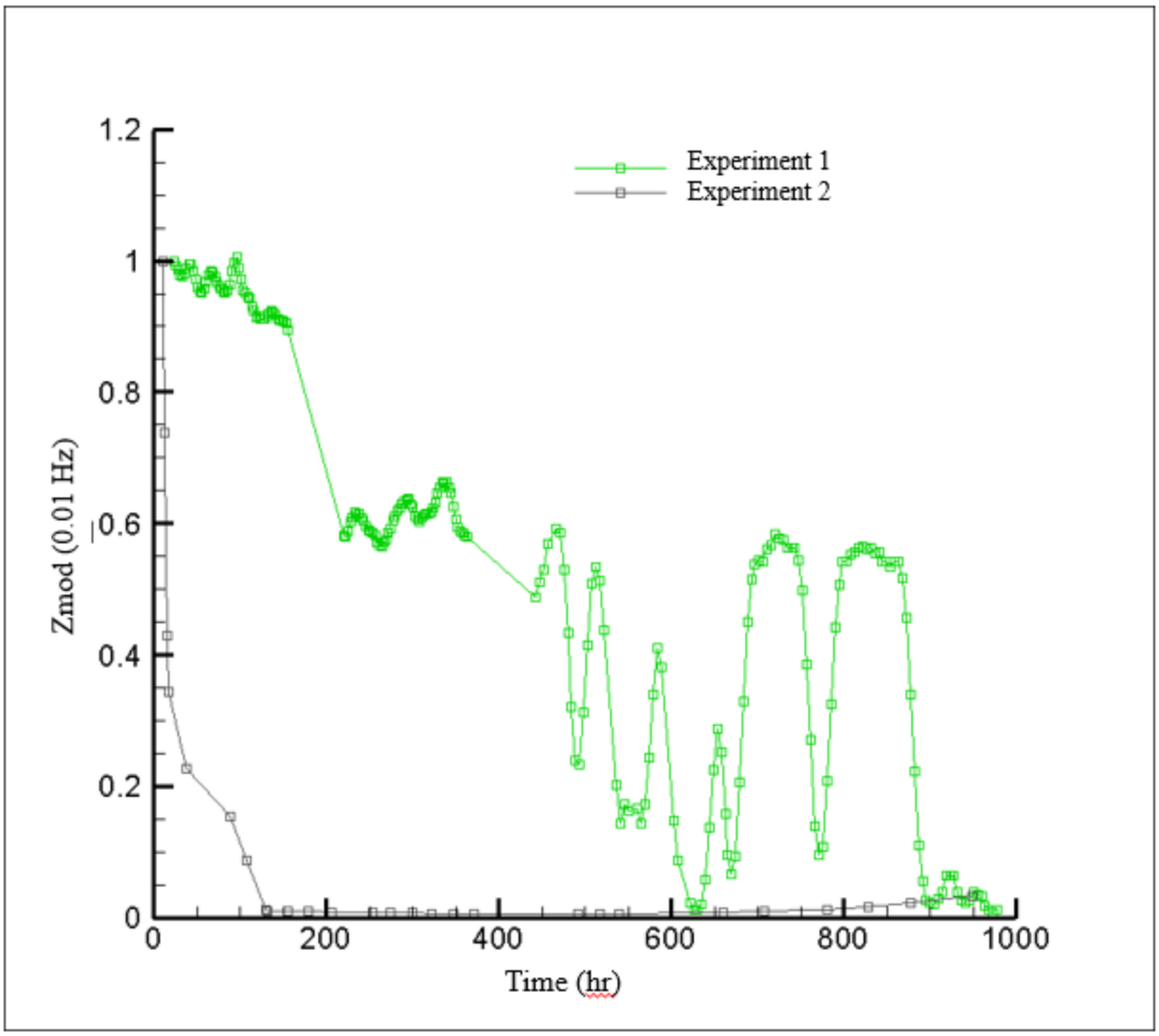

Figure 18. Normalized coating impedance modulus at different flow conditions as a function of time

In Figure 18, Experiment 1 shows the results of a marine coating sample tested in a 90-degree impingement flow at a flow rate of 3.683 cm^3/s. For Experiment 2, the marine coating was tested in a parallel flow apparatus at a flow rate of 3.683 cm^3/s. The impedance data were recorded for both experiments. Then the impedance data at 0.01 Hz frequency was selected and normalized based on the initial data point. The results of both experiments indicate a decrease in impendence during the entire testing cycle. The impedance for a parallel flow showed a much rapid decay than the impedance data from an impingement flow system at the same flow rate.

For the equivalent circuits of the impingement flow system at a 90-degree impact with a flow rate of 3.683 cm^3/s, the coating behavior can be represented as a traditional CPE model shown in Figure 19. A typical CPE model indicates that the failure mechanism is due to the water diffused into the underlayer of the coating. Here R_u is the uncompensated solution resistance, Y_0 is the CPE phase angle, alpha is the CPE exponent, R_p is the polarization resistance. W_d is the Warburg constant. Due to the limitation of the scope of this paper and the focus of device design, we choose not to present the modeling results using the equivalent circuit model.

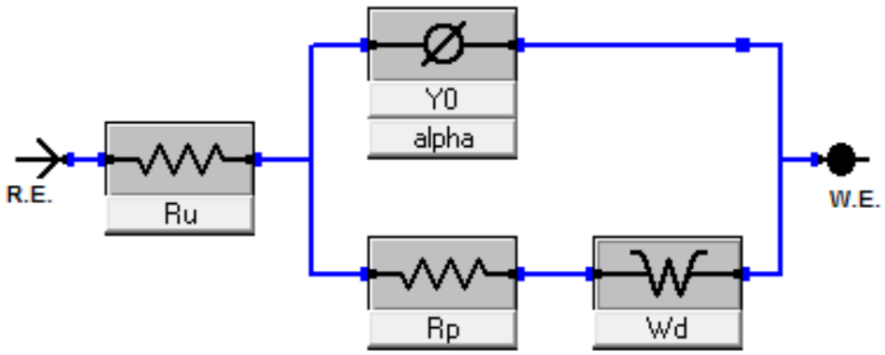

Figure 19. CPE diffusion model for 90-degree impingement flow at a flow rate of 3.683 cm^3/s

CONCLUSION AND FUTURE WORK

In this work, the corrosion degradation of organic coatings under the impingement flow system has been studied. An impingement flow device has been designed and built to help better understand the coating degradation mechanism under different impingement flow conditions through an experimental approach. Electrochemical impedance spectroscopy (EIS) was utilized to quantify and monitor the changes in coating protective quality. A coating degradation test under different impingement flow rates was carried out. The results indicate that organic coating samples have degraded faster at a higher flow rate. By comparing our testing results with a case employing parallel flow, we observed the parallel flow seems to deteriorate the coating sample in a faster manner. However, this is only based on the observation and comparison of one set of data. Through this study, we have proved the robustness of the current impingement flow device and demonstrated the experimental procedures.

Since this paper is mainly focused on the device design. For future work, the focus should shift to the experiment testing. For example, more experiments should be carried out to study the coating degradation under the influence of shear stress and mass transfer rate and their relationship. Furthermore, more tests should be performed to compare the coating degradation differences under different angles of impingement flows. For the organic coating degradation study, the method of topology study is also recommended to investigate the change of surface properties of different regions on the coating surface due to the influence of impingement flow.

REFERENCES

[1] M. J. Schofield, "33 - Corrosion," in *Plant Engineer's Reference Book (Second Edition)*, Second Edi., D. A. Snow, Ed. Oxford: Butterworth-Heinemann, 2002, pp. 25–33.

[2] M. A. Domínguez-Aguilar, M. Díaz-Cruz, A. Cervantes-Tobón, and B. Castro-Domínguez, "The Effect of Jet Flow Impingement on the Corrosion Products Formed on a Pipeline Steel in Naturally Aerated Sour Brine," *J. Mater. Eng. Perform.*, vol. 28, no. 1, pp. 431–447, 2019.

[3] E. Heitz, "Mechanistically based prevention strategies of flow-induced corrosion," *Electrochim. Acta*, vol. 41, no. 4 SPEC. ISS., pp. 503–509, 1996.

[4] NACE, "NACE International," *J. Clin. Eng.*, vol. 35, no. 4, pp. 185–186, 2010.

[5] G2MT Labs, "Cost of Corrosion." [Online]. Available: http://www.g2mtlabs.com/cost-of-corrosion. [Accessed: 12-Dec-2019].

[6] D. A. Jones, *Principles and Prevention Corrosion*, 2nd editio. Person Education (US), 1996.

[7] V. Kain, "Flow accelerated corrosion: Forms, mechanisms and case studies," *Procedia Eng.*, vol. 86, pp. 576–588, 2014.

[8] Y. H. Wei, L. X. Zhang, and W. Ke, "Comparison of the degradation behaviour of fusion-bonded epoxy powder coating systems under flowing and static immersion," *Corros. Sci.*, vol. 48, no. 6, pp. 1449–1461, 2006.

[9] G. P. Bierwagen, "Reflections on corrosion control by organic coatings," *Prog. Org. Coatings*, vol. 28, no. 1, pp. 43–48, 1996.

[10] D. D. MacDonald and M. C. McKubre, "In Electrochemical Corrosion Testing, ASTN STP 727," *ASTM, Philadelphia, PA*, p. 110, 1981.

[11] Q. Le Thu, G. P. Bierwagen, and S. Touzain, "EIS and ENM measurements for three different organic coatings on aluminum," *Prog. Org. Coatings*, vol. 42, no. 3–4, pp. 179–187, 2001.

[12] K. N. Allahar, Q. Su, and G. P. Bierwagen, "In-situ monitoring of organic coatings under QUV/Prohesion exposure by embedded sensors," *NACE - Int. Corros. Conf. Ser.*, no. November, pp. 083931–0839316, 2008.

[13] S. Prochaska and D. Tordonato, *Review of Corrosion Inhibiting Mechanisms in Coatings*, no. September. 2017.

[14] K. Doblhofer and I. Eiselt, "The adhesion and inhibitor properties of organic coatings investigated with very thin polymer films on noble metal electrodes," *Corros. Sci.*, vol. 27, no. 9, pp. 947–956, 1987.

[15] G. Bierwagen, D. Tallman, J. Li, L. He, and C. Jeffcoate, “EIS studies of coated metals in accelerated exposure,” *Prog. Org. Coatings*, vol. 46, no. 2, pp. 149–158, 2003.

[16] O. Haillant, D. Dumbleton, and A. Zielnik, “An Arrhenius approach to estimating organic photovoltaic module weathering acceleration factors,” *Sol. Energy Mater. Sol. Cells*, vol. 95, no. 7, pp. 1889–1895, 2011.

[17] O. Guseva, S. Brunner, and P. Richner, “Service life prediction for aircraft coatings,” *Polym. Degrad. Stab.*, vol. 82, no. 1, pp. 1–13, 2003.

[18] T. Yuzawa, C. Watanabe, S. Tsuge, N. Shimane, and H. Imai, “Application of a pyrolysis-GC/MS system incorporating with micro-UV irradiation to rapid evaluation of the weatherability of acrylic coating paints for house exterior walls,” *Polym. Degrad. Stab.*, vol. 96, no. 1, pp. 91–96, 2011.

[19] M.-G. Olivier *et al.*, “Electrochemical Characterisation of Multilayer Organic Coatings,” *Recent Res. Corros. Eval. Prot.*, vol. 42, no. 2, pp. 1–27, 2012.

[20] G. P. Bierwagen, L. He, J. Li, L. Ellingson, and D. E. Tallman, “Studies of a new accelerated evaluation method for coating corrosion resistance - thermal cycling testing,” *Prog. Org. Coatings*, vol. 39, no. 1, pp. 67–78, 2000.

[21] X. F. Yang, C. Vang, D. E. Tallman, G. P. Bierwagen, S. G. Croll, and S. Rohlik, “Weathering degradation of a polyurethane coating,” *Polym. Degrad. Stab.*, vol. 74, no. 2, pp. 341–351, 2001.

[22] S. Touzain, Q. Le Thu, and G. Bonnet, “Evaluation of thick organic coatings degradation in seawater using cathodic protection and thermally accelerated tests,” *Prog. Org. Coatings*, vol. 52, no. 4, pp. 311–319, 2005.

[23] J. H. Park, G. D. Lee, H. Ooshige, A. Nishikata, and T. Tsuru, “Monitoring of water uptake in organic coatings under cyclic wet-dry condition,” *Corros. Sci.*, vol. 45, no. 8, pp. 1881–1894, 2003.

[24] C. Coatings, R. C. Products, and G. Electrode, “ASTM B117: Standard Practice for Operating Salt Spray (Fog),” *ASTM Stand.*, pp. 1–12, 2011.

[25] M. Molana and S. Banooni, “Investigation of heat transfer processes involved liquid impingement jets: A review,” *Brazilian J. Chem. Eng.*, vol. 30, no. 3, pp. 413–435, 2013.

[26] A. Demoz and T. Dabros, “Relationship between shear stress on the walls of a pipe and an impinging jet,” *Corros. Sci.*, vol. 50, no. 11, pp. 3241–3246, 2008.

[27] K. D. Efird, “Jet Impingement Testing for Flow Accelerated Corrosion,” no. 00129, pp. 0–2, 2000.

[28] M. E. Orazem, J. C. Cardoso Filho, and B. Tribollet, “Application of a submerged impinging jet for corrosion studies: Development of models for the impedance response,” *Electrochim. Acta*, vol. 46, no. 24–25, pp. 3685–3698, 2001.

[29] F. Giralt and O. Trass, “Mass transfer from crystalline surfaces in a turbulent impinging jet. part 2: Erosion and diffusional transfer,” *Can. J. Chem. Eng.*, vol. 54, no. 3, pp. 148–155, 1976.

[30] Gamry Instruments, “Gamry EIS part 1 - The Basics of Electrochemical Impedance Spectroscopy,” 2017.

[31] Q. Zhou, Y. Wang, and G. P. Bierwagen, “Flow accelerated degradation of organic clear coat: The effect of fluid shear,” *Electrochim. Acta*, vol. 142, pp. 25–33, 2014.

[32] J. Wang *et al.*, “Flow-induced corrosion behavior of absorbable magnesium-based stents,” *Acta Biomater.*, vol. 10, no. 12, pp. 5213–5223, 2014.

[33] G. A. Zhang and Y. F. Cheng, “Electrochemical characterization and computational fluid dynamics simulation of flow-accelerated corrosion of X65 steel in a CO2-saturated oilfield formation water,” *Corros. Sci.*, vol. 52, no. 8, pp. 2716–2724, 2010.

[34] M. Metikoš-Huković, R. Babić, I. Škugor Rončević, and Z. Grubač, “Corrosion resistance of copper-nickel alloy under fluid jet impingement,” *Desalination*, vol. 276, no. 1–3, pp. 228–232, 2011.

[35] I. U. Toor, H. M. Irshad, H. M. Badr, and M. A. Samad, “The effect of impingement velocity and angle variation on the erosion corrosion performance of API 5L-X65 carbon steel in a flow loop,” *Metals (Basel).*, vol. 8, no. 6, 2018.

[36] A. R. Hemmati, M. Soltanieh, and S. M. Masoudpanah, “Effect of flow velocity and impact angle on erosion-corrosion behavior of chromium carbide coating,” *J. Tribol.*, vol. 139, no. 3, pp. 1–5, 2017.

[37] Q. Zhou, Y. Wang, and G. P. Bierwagen, “Influence of the composition of working fluids on flow-accelerated organic coating degradation: Deionized water versus electrolyte solution,” *Corros. Sci.*, vol. 55, pp. 97–106, 2012.

[38] S. Yapici, S. Kuslu, C. Ozmetin, H. Ersahan, and T. Pekdemir, “Surface shear stress for a submerged jet impingement using electrochemical technique,” *J. Appl. Electrochem.*, vol. 29, no. 2, pp. 185–190, 1999.

[39] X. Jiang, Y. G. Zheng, and W. Ke, “Effect of flow velocity and entrained sand on inhibition performances of two inhibitors for CO2 corrosion of N80 steel in 3% NaCl solution,” *Corros. Sci.*, vol. 47, no. 11, pp. 2636–2658, 2005.

[40] J. P. Tu, “The effect of TiN coating on erosion-corrosion resistance of α-Ti alloy in saline slurry,” *Corros. Sci.*, vol. 42, no. 1, pp. 147–163, 2000.

[41] M. Bjordal, E. Bardal, T. Rogne, and T. G. Eggen, “Erosion and corrosion properties of WC coatings and duplex stainless steel in sand-containing synthetic sea water,” *Wear*, vol. 186–187, no. PART 2, pp. 508–514, 1995.

[42] M. M. Stack and T. M. Abd El Badia, “Mapping erosion-corrosion of WC/Co-Cr based composite coatings: Particle velocity and applied potential effects,” *Surf. Coatings Technol.*, vol. 201, no. 3–4, pp. 1335–1347, 2006.

[43] A. My, I. Spectra, and E. I. Spectroscopy, “EIS of Organic Coatings and Paints,” *Coating*, vol. 1, pp. 1–7, 2016.

[44] F. Mansfeld, S. L. Jeanjaquet, and M. W. Kendig, “An electrochemical impedance spectroscopy study of reactions at the metal/coating interface,” *Corros. Sci.*, vol. 26, no. 9, pp. 735–742, 1986.

[45] S. Shreepathi, A. K. Guin, S. M. Naik, and M. R. Vattipalli, “Service life prediction of organic coatings: Electrochemical impedance spectroscopy vs actual service life,” *J. Coatings Technol. Res.*, vol. 8, no. 2, pp. 191–200, 2011.

[46] P. Carbonini, T. Monetta, L. Nicodemo, P. Mastronardi, B. Scatteia, and F. Bellucci, “Electrochemical characterisation of multilayer organic coatings,” *Prog. Org. Coatings*, vol. 29, no. 1–4, pp. 13–20, 1996.

[47] Y. Chen, T. Hong, M. Gopal, and W. P. Jepson, “EIS studies of a corrosion inhibitor behavior under multiphase flow conditions,” *Corros. Sci.*, vol. 42, no. 6, pp. 979–990, 2000.

[48] A. S. Shehata, S. A. Nosier, and G. H. Sedahmed, “The role of mass transfer in the flow-induced corrosion of equipments employing decaying swirl flow,” *Chem. Eng. Process.*, vol. 41, no. 8, pp. 659–666, 2002.

[49] J. Villarreal, D. Laverde, and C. Fuentes, “Carbon-steel corrosion in multiphase slug flow and CO2,” *Corros. Sci.*, vol. 48, no. 9, pp. 2363–2379, 2006.

[50] D. Zheng, D. Che, and Y. Liu, “Experimental investigation on gas-liquid two-phase slug flow enhanced carbon dioxide corrosion in vertical upward pipeline,” *Corros. Sci.*, vol. 50, no. 11, pp. 3005–3020, 2008.

[51] L. Y. Xu and Y. F. Cheng, “Effect of fluid hydrodynamics on flow-assisted corrosion of aluminum alloy in ethylene glycol-water solution studied by a microelectrode technique,” *Corros. Sci.*, vol. 51, no. 10, pp. 2330–2335, 2009.

[52] D. Loveday, P. Peterson, and B. Rodgers, “Evaluation of organic coatings with electrochemical impedance spectroscopy: Part 1: Fundamentals of electrochemical impedance spectroscopy,” *CoatingsTech*, vol. 1, no. 8, pp. 46–52, 2004.